ORGANOMETALLICS

pubs.acs.org/Organometallics Article

Synthesis and Characterization of Rh^{III}–M^{II} (M = Pt, Pd) Heterobimetallic Complexes Based on a Bisphosphine Ligand: Tandem Reactions Using Ethanol

Zeinab Mandegani,[‖] Asma Nahaei,[‖] Mahshid Nikravesh, S. Masoud Nabavizadeh,* Hamid R. Shahsavari,* and Mahdi M. Abu-Omar*

Cite This: https://dx.doi.org/10.1021/acs.organomet.0c00594 Read Online

ABSTRACT: 1,1-Bis(diphenylphosphino)methane (dppm) was used as a linker ligand for the preparation of a series of heterobimetallic Rh^{III}–Pt^{II} and Rh^{III}–Pd^{II} complexes. These complexes were characterized by means of several analytical and spectroscopic methods. The catalytic activities of these heterobimetallic complexes were carried out in three different tandem reactions: namely, transfer hydrogenation (TH)/dehalogenation (DH), TH/Suzuki–Miyaura coupling, and coupling of benzylic alcohols with nitrobenzenes for Schiff base construction. Ethanol was used as both the solvent and an inexpensive TH reagent, where a broad substrate scope was demonstrated for these tandem reactions. All reactions proceeded smoothly in air at 80–90 °C. The Rh^{III}–Pd^{II} complex showed superior catalytic performance in comparison to the Rh^{III}–Pt^{II} complexes, its monometallic counterparts, and mixtures of monometallic (Rh^{III} + Pd^{II}) complexes. The result demonstrates a cooperative effect between the Rh and Pd metal centers. A mechanism for the catalytic tandem reactions was investigated. It was found that alcohol medium and base are essential.

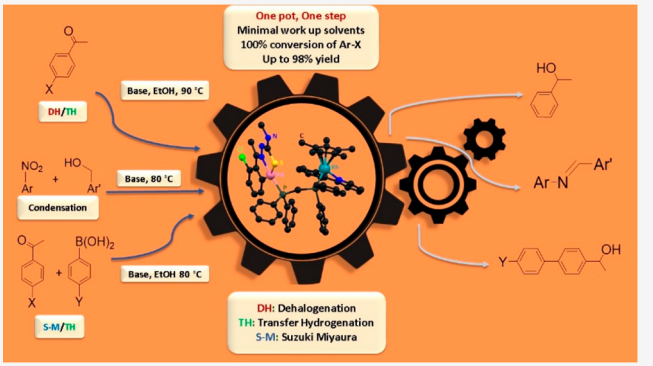

INTRODUCTION

The discovery of efficient catalytic systems continues to be a challenge in homo- and heterogeneous catalysis in organic synthesis.[1−3] From this viewpoint, heterobimetallic systems have emerged as a new platform in catalysis.[4−10] These have been considered in various aspects of catalysis research with applications in biomimetic catalysis,[11,12] tandem reactions,[5,13] olefin hydrogenation,[14,15] N_2 fixation,[16,17] and H_2 activation.[15,18,19] Because bimetallic complexes incorporate more than one metal center, they exhibit unusual reactivity and potential synergy in catalysis. Cooperative electronic and steric effects between the metal centers and/or coordinated ligands may arise.[5,20,21]

The preparation of heterobimetallic complexes could be challenging and requires a rational synthetic approach concerning the compatibility and stability of the ligands and metals.[22−24] Consequently, if the two metal complexes have enough stability, first they can be synthesized individually and subsequently combined. Correspondingly, further purification can be avoided using this approach.[25] In a second synthetic strategy, bifunctional chelating ligands can be used to impose selective coordination to each metal center. This method is challenging when similar metals are applied.[26] A stepwise

Chart 1. Examples of Heterobimetallic Complexes

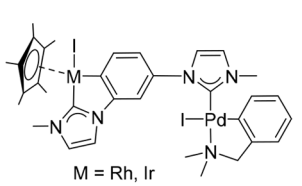

Organometallics, 2019, 38, 2120-2131

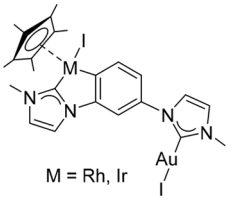

Organometallics, 2018, 37, 4092-4099

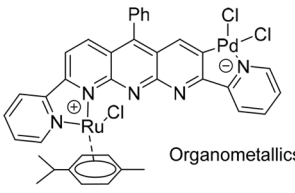

Organometallics, 2020, 39, 123-131

Received: September 7, 2020

https://dx.doi.org/10.1021/acs.organomet.0c00594
Organometallics XXXX, XXX, XXX−XXX

synthetic pathway could yet be another alternative method for the preparation of heterobimetallic complexes. In this approach, a metal complex is prepared and a ditopic bridging ligand (a donor ligand possessing two binding sites for the coordination to metal atoms) is bound to the first metal, which is followed by coordination of the second metal complex.[27] Among these linker ligands, 1,1-bis(diphenylphosphino)methane (dppm) is a suitable candidate for the coordination of various metals to form homo- and heterobimetallic complexes.[28] This ligand has a short chain between its two phosphine moieties which can hold the metal centers close to each other. Sometimes this proximity leads to metal−metal bond formation. Also, we have widely engaged the dppm ligand as a bridging ligand for the formation of homo- and hetero-organoplatinum complexes with different applications.[29−33]

Tandem catalysis refers to the combination of two steps in one, which makes the process shorter and saves energy, as the interim purification is avoided.[34] Additionally, the usage of one-pot multistep reactions has been reported as an important and effective pathway for the construction of C−N[35,36] and C−C bonds[20,37] or activation of C−F,[38,39] and C−H bonds[38,40] in organic synthesis. Heterobimetallic compounds can be an option for tandem catalytic processes.[5] In this regard, several catalytic systems such as Ir^{III}−Pd^{II},[35,37,41] Rh^{III}−Pd^{II},[37,41] Ru^{II}−Pd^{II},[13,41] Ir^{III}−Au^{I},[42] Rh^{III}−Au^{I},[42] Pd^{II}−Au^{I},[43,44] etc. have been described and their catalytic activities investigated in various tandem transformations (Chart 1).

We have synthesized and characterized new Rh^{III}−Pt^{II} and Rh^{III}−Pd^{II} complexes supported by a dppm bridging ligand. The Rh^{III}−Pd^{II} complex showed good catalytic activity in three tandem reactions: (i) transfer hydrogenation (TH) and dehalogenation (DH), (ii) TH and Suzuki−Miyaura coupling, and (iii) nitro reduction and imine preparation. Interestingly, in our tandem reactions ethanol (having abundance, sustainability, and a safe nature) was used as a powerful and efficient hydrogen source for the tandem reactions. Although formic acid or ^{i}PrOH have been mainly used for TH reactions,[37,41] ethanol has rarely been applied for tandem processes.[45−48] This difficulty can be attributed to the fact that EtOH causes catalyst deactivation.[46,47]

EXPERIMENTAL SECTION

General Information. All chemicals were purchased from Sigma-Aldrich or Merck and were used without any further purification. NMR spectra were recorded on a Bruker Avance DPX 400 MHz spectrometer at room temperature; frequencies are referenced to Me_4Si (^{1}H and ^{13}C{^{1}H}), 85% H_3PO_4 (^{31}P{^{1}H}), and Na_2PtCl_6 (^{195}Pt{^{1}H}). The chemical shifts and coupling constants are given in ppm and Hz, respectively. Microanalyses were done using a Thermo Finnigan Flash EA-1112 CHNSO rapid elemental analyzer. Mass data were obtained by a time-of-flight mass spectrometer equipped with an electrospray ion source (Bruker micrOTOF II). UV−vis absorption spectra were recorded on a PerkinElmer Lambda 25 spectrophotometer using a cuvette with 1.00 cm path length. Powder X-ray diffraction (PXRD) spectra were recorded on a Bruker AXS D8-Advance X-ray diffractometer with Cu Kα radiation (λ = 1.5418 Å). All yields refer to the isolated products. The known precursor complexes [{Ag(CH$_3$CN)$_4$}PF$_6$],[49] [Cp*Rh(ppy)Cl][50] (Cp* = pentamethylcyclopentadienyl; ppy = 2-phenylpyridnate), [Cp*{Rh(ppy)(CH$_3$CN)}PF$_6$] (**1**),[51] [PtMe(Obpy)(κ^1-dppm)] (**2a**;[52] Obpy = 2,2′-bipyridine *N*-oxide), [Pt(*p*-MeC$_6$H$_4$)(ppy)(κ^1-dppm)] (**2b**),[31] and [Pd(TSC)(κ^1-dppm)] (**2c**;[53] TSC = 2-chlorophenyl thiosemicarbazone) were prepared by literature methods.

Synthesis of Complexes. *[{Cp*Rh(ppy)(CH$_3$CN)}PF$_6$] (**1**).* This complex was prepared by a modified procedure.[51] Under dark conditions and an Ar atmosphere, [{Ag(CH$_3$CN)$_4$}PF$_6$] (97 mg, 0.23 mmol) was added to a solution of [Cp*Rh(ppy)Cl] (100 mg, 0.23 mmol) in CH_2Cl_2 (10 mL). The resulting mixture was stirred at room temperature for 1 h. The reaction mixture was filtered on Celite to separate the AgCl precipitate. The solvent of the orange solution was reduced to a small volume, and 3 mL of *n*-hexane was added; afterward **1** was precipitated as a light orange solid. Yield: 93%. The NMR spectral data agree with those reported in the literature.[51]

*[{Cp*Rh(ppy)(μ-dppm)PtMe(Obpy)}PF$_6$] (**3a**).* Under an Ar atmosphere, **1** (58 mg, 0.1 mmol) and **2a** (77 mg, 0.1 mmol) were dissolved in CH_2Cl_2 (10 mL) to give an orange solution that was stirred at room temperature for 2 h. The solvent was reduced to a small volume, and 3 mL of *n*-pentane was added; afterward **3a** was precipitated as an orange solid. Yield: 86%. Anal. Calcd for $C_{57}H_{55}F_6N_3OP_3PtRh$ (MW = 1302.96): C, 52.54; H, 4.25; N, 3.22. Found: C, 52.19; H, 4.34; N, 3.46. HR ESI-MS(+): *m*/*z* calcd for $C_{46}H_{45}NP_2Rh$ [**4** − PF$_6$]$^+$ 776.2; found 776.2. NMR in CD$_3$CN: δ (^{1}H, 400 MHz) 0.94 (d, $^2J_{PtH}$ = 77.8 Hz, $^3J_{PH}$ = 7.0 Hz, 3H, PtMe), 1.62 (s, 15H, MeCp*), 3.67 (t, $^3J_{PtH}$ = 26.1 Hz, $^2J_{PH}$ = 10.6 Hz, 2H, CH$_2$ of dppm), 6.84 (t, $^3J_{HH}$ = 5.9 Hz, 1H), 7.20 (t, $^3J_{HH}$ = 7.5 Hz, 1H), 7.23−7.45 (m, 17 H), 7.48−7.54 (m, 4H), 7.56−7.66 (m, 4H), 7.75−7.86 (m, 2H), 7.94−8.03 (m, 3H), 8.09 (d, $^3J_{PtH}$ = 21.7 Hz, $^3J_{HH}$ = 6.1 Hz, 1H), 8.76 (d, $^3J_{HH}$ = 5.6 Hz, 1H), 9.90 (d, $^3J_{HH}$ = 8.1 Hz, 1H); δ (^{31}P{^{1}H}, 162 MHz) 25.0 (d, $^1J_{PtP^1}$ = 2209 Hz, $^2J_{P^1P^2}$ = 96 Hz, P^1), 0.3 and −3.6 (dd, $^1J_{RhP^2} \approx$ 46 Hz, $^3J_{PtP^2} \approx$ 312 Hz, $^2J_{P^1P^2}$ = 96 Hz, P^2), −144.6 (septet, $^1J_{P^3F}$ = 707 Hz, PF$_6$); δ (^{195}Pt{^{1}H}, 85 MHz) −3986.2 (dt, $^1J_{PtP^1}$ = 2212 Hz, $^1J_{PtP^2}$ = 314 Hz).

*[{Cp*Rh(ppy)(μ-dppm)Pt(p-MeC$_6$H$_4$)(ppy)}PF$_6$] (**3b**).* This compound was made similarly to **3a** using **2b**. Yield: 74%. Anal. Calcd for $C_{64}H_{60}F_6N_2P_3PtRh$ (MW = 1362.07): C, 56.44; H, 4.44; N, 2.06. Found: C, 56.71; H, 4.47; N, 2.24. HR ESI-MS(+): *m*/*z* calcd for $C_{46}H_{45}NP_2Rh$ [**4** − PF$_6$]$^+$ 776.2; found 776.2. NMR in CD$_3$CN: δ (^{1}H, 400 MHz) 1.62 (s, 15H, MeCp*), 1.99 (s, 3H, Me of *p*-MeC$_6$H$_4$), 2.94 (t, $^3J_{PtH}$ = 21.8 Hz, $^2J_{PH}$ = 9.8 Hz, 2H, CH$_2$ of dppm), 6.27 (d, $^3J_{HH}$ = 7.7 Hz, 2H), 6.78 (td, $^3J_{HH}$ = 7.1, $^4J_{HH}$ = 1.7 Hz, 1H) 7.16−7.27 (m, 18H), 7.31−7.38 (m, 5H), 7.40 (td, $^3J_{HH}$ = 7.3, $^4J_{HH}$ = 2.1 Hz, 1H), 7.55−7.68 (m, 4H), 7.71−7.85 (m, 4H), 7.95−8.00 (m, 3H), 8.12 (d, $^3J_{PtH}$ = 19.2, $^3J_{HH}$ = 5.5 Hz, 1H), 8.76 (d, $^3J_{HH}$ = 5.6 Hz, 1H); δ (^{31}P{^{1}H}, 162 MHz) 23.9 (d, $^1J_{PtP^1}$ = 1896 Hz, $^2J_{P^1P^2}$ = 93 Hz, P^1), − 2.2 and −6.1 (dd, $^1J_{RhP^2} \approx$ 39 Hz, $^3J_{PtP^2} \approx$ 291 Hz, $^2J_{P^1P^2}$ = 93 Hz, P^2), − 144.6 (septet, $^1J_{P^3F}$ = 707 Hz, PF$_6$); δ (^{195}Pt{^{1}H}, 85 MHz) −3831.2 (dt, $^1J_{PtP^1}$ = 1892 Hz, $^1J_{PtP^2}$ = 294 Hz).

*[{Cp*Rh(ppy)(μ-dppm)Pd(TSC)}PF$_6$] (**3c**).* This compound was made similarly to **3a** using **2c**. Yield: 81%. Anal. Calcd for $C_{56}H_{55}ClF_6N_4P_3PdRhS$ (MW = 1267.82): C, 53.05; H, 4.37; N, 4.42; S, 2.53. Found: C, 53.21; H, 4.31; N, 4.57; S, 2.62. HR ESI-MS(+): *m*/*z* calcd for $C_{46}H_{45}NP_2Rh$ [**4** − PF$_6$]$^+$ 776.2; found 776.2. NMR in CDCl$_3$: δ (^{1}H, 400 MHz) 1.74 (s, 15H, MeCp*), 2.73 (s, 3H, MeC═N), 2.94 (d, $^3J_{HH}$ = 4.9 Hz, 3H, NH*Me*), 4.15 (t, $^2J_{PH}$ = 9.2 Hz, 2H, CH$_2$ of dppm), 3.98 (br, 1H, N*H*Me), 6.73 (t, $^3J_{HH}$ = 7.6 Hz, 1H), 6.80 (t, $^3J_{HH}$ = 7.7 Hz, 1H), 7.11−7.20 (m, 15H), 7.38 (d, $^3J_{HH}$ = 7.5 Hz, 1H), 7.43−7.51 (m, 8H), 7.63 (d, $^3J_{HH}$ = 8.0 Hz, 1H), 7.76−7.84 (m, 3H), 8.69 (d, $^3J_{HH}$ = 5.2 Hz, 1H); δ (^{31}P{^{1}H}, 162 MHz) 30.7 (dd, $^1J_{RhP^1}$ = 151 Hz, $^2J_{P^1P^2}$ = 28 Hz, P^1), 22.0 (dd, $^3J_{RhP^2}$ = 4 Hz with $^2J_{P^1P^2}$ = 28 Hz, P^2), − 144.1 (septet, $^1J_{P^3F}$ = 711 Hz, PF$_6$).

*[{Cp*Rh(ppy)(μ-dppm)}PF$_6$] (**4**).* Under an Ar atmosphere, **1** (58 mg, 0.1 mmol) and the dppm ligand (39 mg, 0.1 mmol), in a 1:1 molar ratio, were dissolved in CH_2Cl_2 (10 mL) to give a dark orange solution that was stirred at room temperature for 1 h. The solvent was reduced to a small volume, and 3 mL of *n*-pentane was added; afterward **4** was precipitated as an orange solid. Yield: 94%. Anal. Calcd for $C_{46}H_{45}F_6NP_3Rh$ (MW = 921.67): C, 59.94; H, 4.92; N, 1.52. Found: C, 59.83; H, 4.93; N, 1.61. HR ESI-MS(+): *m*/*z* calcd for $C_{46}H_{45}NP_2Rh$ [**4** − PF$_6$]$^+$ 776.2; found 776.2. NMR in CDCl$_3$: δ (^{1}H, 400 MHz) 1.43 (s, 15H, MeCp*), 2.08 ppm (dd, $^1J_{HH}$ = 14.6 Hz, $^2J_{PH}$ = 8.6 Hz, 1H, CH$_2$ of dppm), 2.27 (dd, $^1J_{HH}$ = 14.6 Hz, $^2J_{PH}$ = 10.2 Hz, 1H, CH$_2$ of dppm), 6.69 (t, $^3J_{HH}$ = 7.6 Hz, 1H), 6.77 (t, $^3J_{HH}$ = 7.7 Hz, 1H), 7.04 (t, $^3J_{HH}$ = 7.8 Hz, 1H), 7.09−7.20 (m, 20H), 7.39 (d, $^3J_{HH}$ = 7.7 Hz, 1H), 7.47 (d, $^3J_{HH}$ = 7.8 Hz, 1H), 7.64 (d, $^3J_{HH}$ = 8.0 Hz, 1H), 7.79 (t, $^3J_{HH}$ = 7.7 Hz, 1H), 8.69 (d, $^3J_{HH}$ = 5.4 Hz, 1H); δ (^{31}P{^{1}H},

https://dx.doi.org/10.1021/acs.organomet.0c00594
Organometallics XXXX, XXX, XXX−XXX

Scheme 1. Synthetic Routes for Preparation of Heterobimetallic Rh^{III}–M^{II} (M = Pt (a), Pd (b)) Complexes 3, with P Atom Numbering

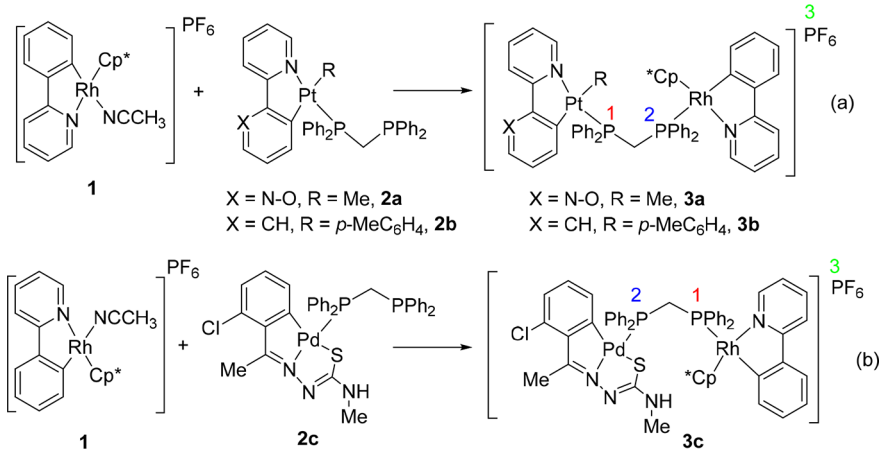

162 MHz) 31.9 (dd, $^1J_{RhP}{}^1$ = 148 Hz, $^2J_{P^1P^2}$ = 54 Hz, P^1), − 29.3 (d, $^2J_{P^1P^2}$ = 54 Hz, P^2), − 144.1 (septet, $^1J_{P^3F}$ = 713 Hz, PF_6).

Catalytic Investigation. *Transfer Hydrogenation/Dehalogenation of p-Haloacetophenones.* A capped vessel containing a stir bar was charged with the corresponding *p*-haloacetophenone (1 mmol), Cs_2CO_3 (2 mmol), catalyst (2 mol %), and EtOH (2 mL). The reaction mixture was stirred at 90 °C for an appropriate amount of time. Reaction monitoring, yields, and conversions were determined by TLC chromatography. Isolated products were characterized by ^1H and $^{13}C\{^1H\}$ NMR after plate chromatography purification using *n*-hexane:ethyl acetate (9:1).

Transfer Hydrogenation/Suzuki–Miyaura Coupling. A capped vessel containing a stir bar was charged with 4-haloacetophenone (0.36 mmol), arylboronic acid (0.55 mmol), Cs_2CO_3 (1.08 mmol), catalyst **3** (2 mol %), and 2 mL of alcohol, and the solution was heated to 80 °C for an appropriate amount of time. Products were characterized by ^1H and $^{13}C\{^1H\}$ NMR after plate chromatography purification using *n*-hexane:ethyl acetate (10:2).

Condensation of Nitroarenes and Primary Alcohols. A capped vessel containing a stir bar was charged with nitrobenzene (0.3 mmol), benzyl alcohol (5.0 mmol), Cs_2CO_3 (0.3 mmol), and catalyst (2 mol %). The solution was heated to 80 °C for an appropriate amount of time. Products were characterized by ^1H and $^{13}C\{^1H\}$ NMR after plate chromatography purification using *n*-hexane:ethyl acetate (8:2).

Computational Details. All calculations were performed using Gaussian 16 software.[54] The B3LYP functional was used in combination with the 6-31G(d) basis set for all main-group elements, except for Pd and Rh, for which the LANL2DZ basis set was used.[55] The energies were calculated by the CPCM model in EtOH solution. The Cartesian coordinates and energies of the optimized structures are reported in the Supporting Information. The calculations for the electronic absorption spectra using TD-DFT were performed at the same level of theory. The compositions of molecular orbitals and theoretical absorption spectra were plotted using Chemissian software.[56]

Crystallographic Data. Single-crystal X-ray diffraction data for **1** were collected on a Bruker KAPPA APEX II diffractometer equipped with an APEX II CCD detector using a TRIUMPH monochromator with a Mo Kα X-ray source (λ = 0.71073 Å). The crystal was mounted on a cryoloop under Paratone-N oil and kept under nitrogen. Absorption correction of the data was carried out using the multiscan method SADABS.[57] Subsequent calculations were carried out using SHELXTL.[58] Structure determination was done using intrinsic methods. Structure solution, refinement, and creation of publication data were performed using SHELXTL. Crystallographic information is presented in Table S1.

RESULTS AND DISCUSSION

Synthesis and Characterization of Compounds. The heterobimetallic Rh^{III}–Pt^{II} complexes [{Cp*Rh(ppy)(μ-dppm)PtR(C∧N)}PF_6] (**3a,b**; Cp* = pentamethylcyclopentadienyl; ppy = 2-phenylpyridnate, Obpy = 2,2′-bipyridine *N*-oxide; **3a**, R = Me, C∧N = Obpy; **3b**, R = *p*-MeC_6H_4, C∧N = ppy) and the Rh^{III}–Pd^{II} complex [{Cp*Rh(ppy)(μ-dppm)Pd(TSC)}PF_6] (**3c**; TSC = 2−chlorophenyl thiosemicarbazone) were prepared by the stepwise procedure depicted in Scheme 1.

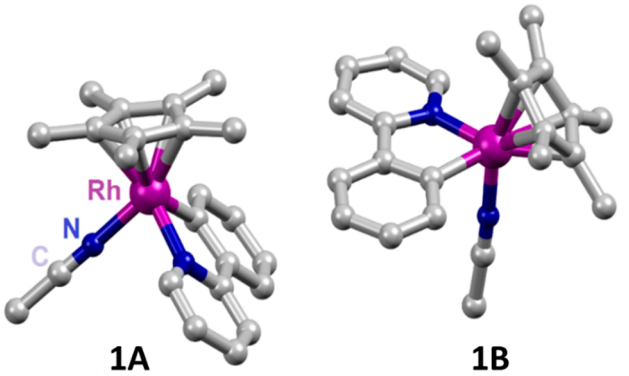

Figure 1. ORTEP view of the two molecules (**1A**,**B**) in the asymmetric unit of **1**. Ellipsoids are drawn at the 50% probability level. The PF_6 groups have been omitted for clarity.

The starting monometallic Pt^{II} complexes [PtMe(Obpy)(κ^1-dppm)] (**2a**)[52] and [Pt(*p*-MeC_6H_4)(ppy)(κ^1-dppm)] (**2b**)[31] and the Pd^{II} complex [Pd(TSC)(κ^1-dppm)] (**2c**)[53] were synthesized according to previously described methods. These complexes were obtained in high yield and characterized by means of NMR spectroscopy.

The monometallic Rh^{III} compound [{Cp*Rh(ppy)-(CH_3CN)}PF_6] (**1**) was prepared by a modification of the already published procedure.[51] The Preparation of complex **1** generated by treating [{Ag(CH_3CN)$_4$}PF_6][49] and [Cp*Rh-(ppy)Cl][50] in CH_2Cl_2 was shown to be an improved and efficient method (reaction rate and yield) relative to the prior report.[51] The structure of **1** was determined using NMR and X-ray techniques. The appropriate crystals of **1** were grown by slow evaporation of a $CHCl_3$ solution of this complex at room temperature. This complex crystallized in the monoclinic crystal

https://dx.doi.org/10.1021/acs.organomet.0c00594
Organometallics XXXX, XXX, XXX−XXX

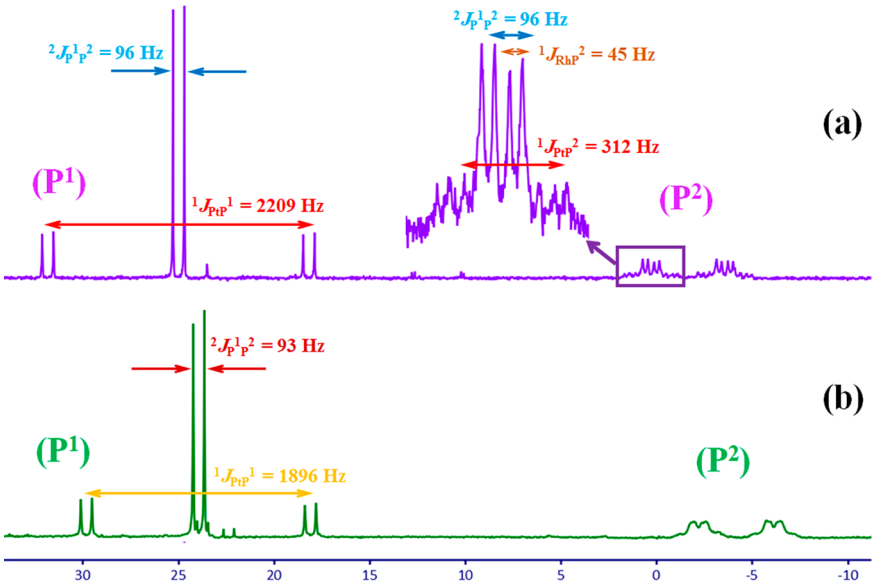

Figure 2. $^{31}P\{^1H\}$ NMR spectra of (a) **3a** and (b) **3b** in CD_3CN at room temperature.

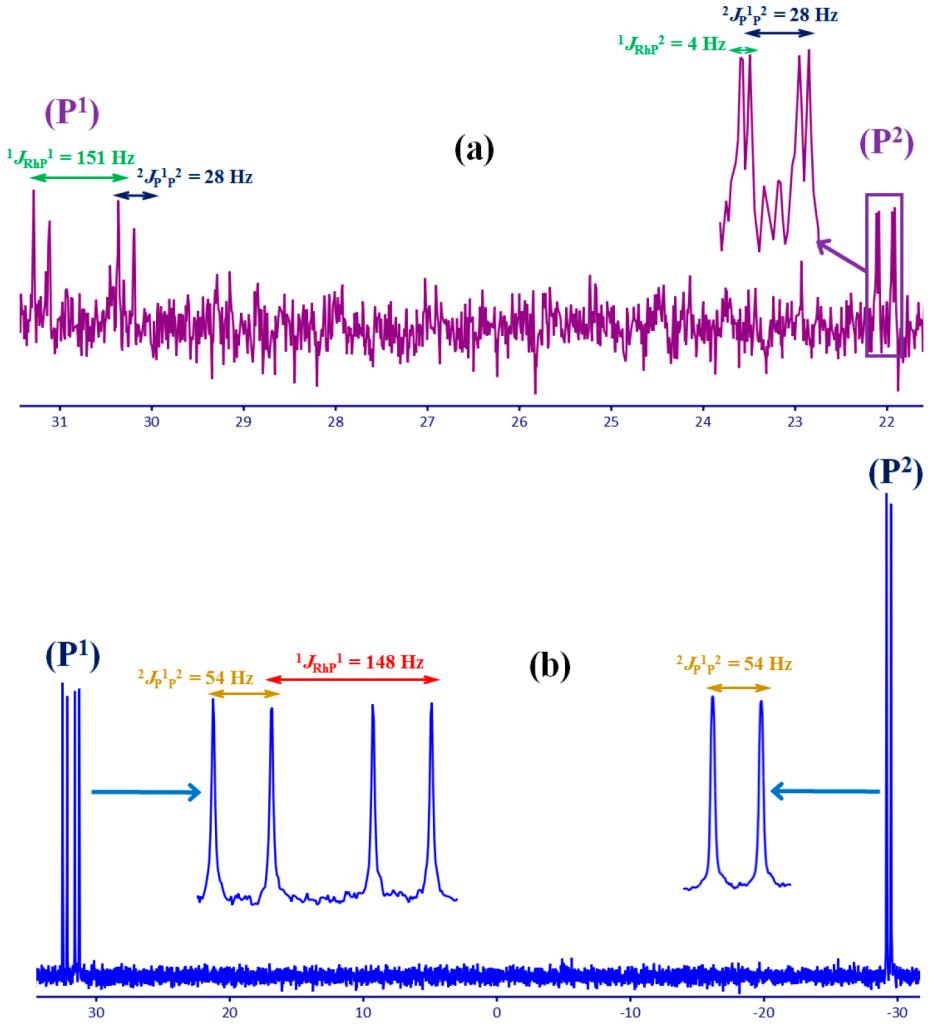

Figure 3. $^{31}P\{^1H\}$ NMR spectra of (a) **3c** and (b) **4** in $CDCl_3$, at room temperature.

system and space group $P2_1/c$, and the crystal structure of **1** contains two molecules in the asymmetric unit cell. An ORTEP view of **1** is illustrated in Figure 1, while the crystal data and structural refinement parameters and the main bond lengths and angles of **1** (molecule **1A**) are summarized in Tables S1 and S2, respectively. The structure of **1** displays a piano-stool type

https://dx.doi.org/10.1021/acs.organomet.0c00594
Organometallics XXXX, XXX, XXX−XXX

Scheme 2. Synthetic Pathway for the Preparation of 4, with P Atom Numbering

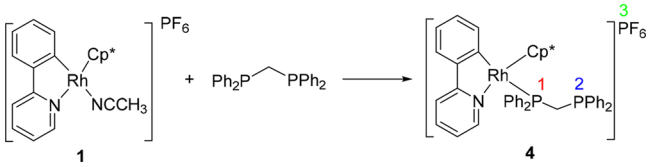

1 4

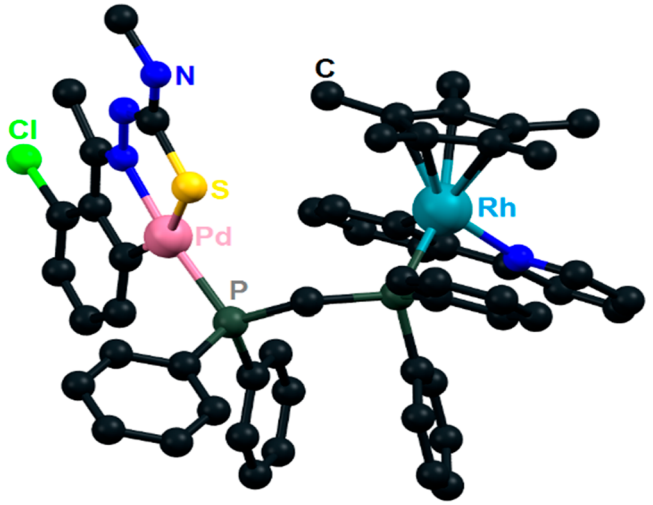

Figure 4. Optimized structure of **3c**. H atoms are omitted for clarity.

geometry, and the bond lengths for this complex are in the range found for other similar Rh^{III} complexes.[50,51,59,60]

The treatment of **1** with **2a−c** in stoichiometric amounts led to the formation of **3a−c**. In complexes **2**, the dppm ligand acts as a monodentate pendant ligand and it can easily bind to **1** by replacement of the weakly coordinated CH_3CN ligand to give complexes **3** in high yields. The integrity of **3** in solution was confirmed by multinuclear NMR spectroscopy. In the $^{31}P\{^1H\}$ NMR spectra of Pt−Rh complexes, two distinct resonances are observed for the dppm ligand at different frequencies (Figure 2). For P^1 (coordinated to the platinum center) in **3a** and **3b**, a signal appeared as a doublet at δ 25.0 ppm with $^1J_{PtP^1}$ = 2209 Hz and $^2J_{P^1P^2}$ = 96 Hz and a doublet at δ 23.9 ppm with $^1J_{PtP^1}$ = 1896 Hz, $^2J_{P^1P^2}$ = 93 Hz, respectively. The lower coupling constant between platinum and phosphorus in **3b** is related to the high *trans* influence of the carbon of the ppy ligand in comparison to the Obpy ligand. Interestingly, in these complexes for P^2 (coordinated to rhodium center) two signals are observed as a doublet of doublets at δ 0.3 and −3.6 ppm, each with $^1J_{RhP^2} \approx 46$ Hz, $^3J_{PtP^2} \approx 312$ Hz, and $^2J_{P^1P^2}$ = 96 Hz for **3a** and a doublet of doublets at δ −2.2 and −6.1 ppm, with $^1J_{RhP^2} \approx 39$ Hz, $^3J_{PtP^2} \approx 291$ Hz, and $^2J_{P^1P^2}$ = 93 Hz for **3b**. This observation perhaps is relevant to the disposition of the different ligands on the Rh center, which results in chirality on the rhodium moiety.[61−63] Also, for **3c** two different doublet of doublets for both P ligating atoms at δ 30.7 ppm with $^1J_{RhP^1}$ = 151 Hz and $^2J_{P^1P^2}$ = 28 Hz and at δ 22.0 ppm with $^3J_{RhP^2}$ = 4 Hz and $^2J_{P^1P^2}$ = 28 Hz are observed (Figure 3). A septet signal for the PF_6^- counterion at a lower chemical shift appeared for all complexes at δ −144.6 ppm with $^1J_{P^3F}$ = 707 Hz for **3a**,**b** and at δ −144.1 ppm with $^1J_{P^3F}$ = 711 Hz for **3c**. In these spectra a substantial chemical shift change was detected for the free phosphine in **2** (doublet at δ −26.3 ppm with $^3J_{PtP^2}$ = 54 Hz and $^2J_{P^1P^2}$ = 91 Hz for **2a**; doublet at δ −28.6 ppm with $^3J_{PtP^2}$ = 48 Hz, $^2J_{P^1P^2}$ = 50 Hz for **2b**; doublet at δ −26.7

Table 1. Tandem Reaction (TH/DH) of *p*-Haloacetophenones[a]

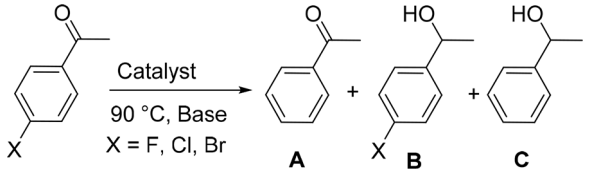

entry	catalyst	X	base	time (h)	yield (%)[b] A	B	C	TON
1	**2c**	Cl	Cs_2CO_3	24	30	10	-	150
2	**2c**	Cl	NaO^tBu	24	45	15	-	300
3	**2c**[c]	Cl	Cs_2CO_3	24	40	10	-	250
4	**2c**	Br	Cs_2CO_3	24	10	-	40	200
5	**2c**	F	Cs_2CO_3	24	-	60	-	250
6	**1**	Cl	Cs_2CO_3	24	10	40	-	300
7	**1**	Cl	NaO^tBu	24	10	45	-	275
8	**1**[c]	Cl	Cs_2CO_3	24	10	40	-	250
9	**1**	Br	Cs_2CO_3	24	40	-	10	250
10	**1**	F	Cs_2CO_3	24	-	70	-	400
11	**1** + **2c**	Br	Cs_2CO_3	24	15	-	53	340
12	**3c**	Cl	Cs_2CO_3	15	trace	trace	90	450
13	**3c**[c]	Cl	Cs_2CO_3	15	trace	trace	70	350
14	**3c**	Br	Cs_2CO_3	8	-	-	96	480
15	**3c**	F	Cs_2CO_3	10	-	-	-	0
16	**3c**	F	NaO^tBu	8	-	80	-	400
17	**4**	Br	Cs_2CO_3	24	-	70	10	350
18	**4**	F	Cs_2CO_3	24	-	80	-	400
19	**3a**[c]	Br	Cs_2CO_3	48	trace	trace	-	0
20	**3a**[d]	Br	Cs_2CO_3	48	10	45	-	275
21	**3a**[c]	Br	NaO^tBu	48	-	trace	-	0
22	**3a**[d]	Br	NaO^tBu	48	-	15	-	75
23	**3b**[c]	Br	Cs_2CO_3	48	-	trace	-	0
24	**3b**[c]	Br	NaO^tBu	48	-	trace	-	0
25	**3b**[d]	Br	NaO^tBu	48	-	trace	-	0

[a]Reaction conditions unless specified otherwise: *p*-haloacetophenone (1 mmol), base (2 mmol), catalyst (2 mol %), and 2 mL of ethanol, 90 °C. [b]Isolated yields after preparatory thin-layer plate chromatography. [c]Ethanol as the solvent, 110 °C. [d]^{i}PrOH as the solvent, 110 °C.

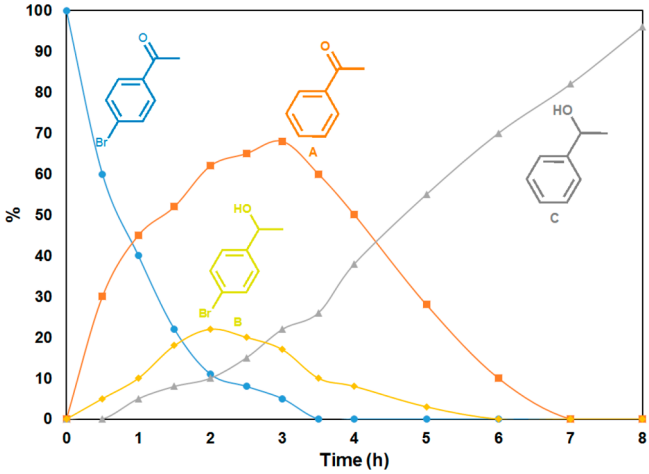

Figure 5. Reaction profile for the TH/DH of *p*-bromoacetophenone (1 mmol) and **3c** (2 mol %) in the presence of Cs_2CO_3 (2 mmol) and EtOH (2 mL) at 90 °C.

https://dx.doi.org/10.1021/acs.organomet.0c00594
Organometallics XXXX, XXX, XXX−XXX

Scheme 3. Proposed Mechanism for the TH/DH Reaction

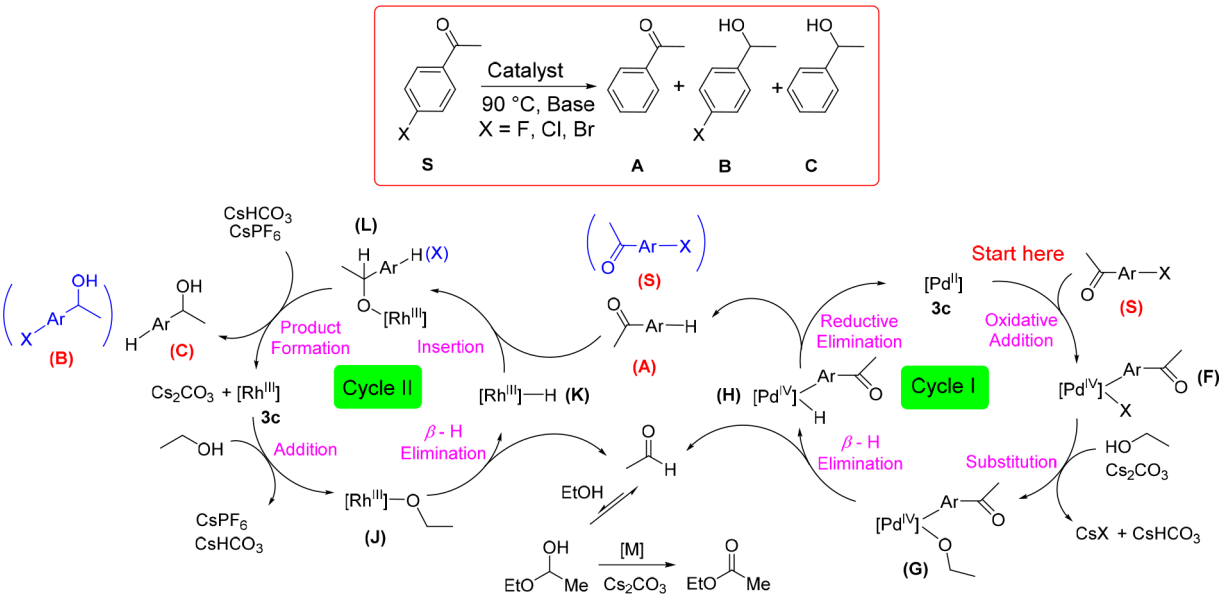

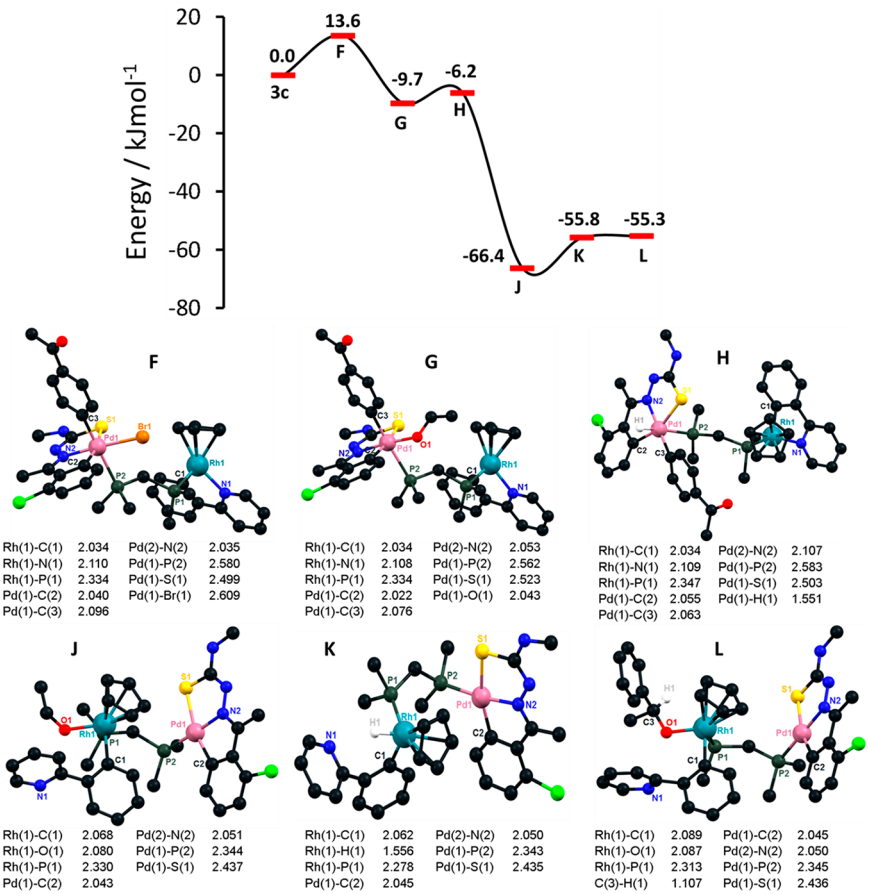

Figure 6. Relative energy profile and DFT-calculated proposed structures of intermediates **F**−**H** and **J**−**L**. Selected bond lengths (Å) are also shown.

ppm with $^2J_{P^1P^2}$ = 79 Hz for **2c**) to **3**. This downfield chemical shift is related to the coordination of rhodium to the free phosphine,[29,31] and it revealed a considerable coupling constant between Rh and P^2 in **3**. The $^{195}Pt\{^1H\}$ NMR spectra of Pt−Rh complexes contain a pseudo doublet of triplets arising from the coupling between the platinum center and phosphorus (δ −3986.2 ppm with $^1J_{PtP^1}$ = 2212 Hz and $^1J_{PtP^2}$ = 314 Hz, **3a**; δ −3831.2 ppm with $^1J_{PtP^1}$ = 1892 Hzand $^1J_{PtP^2}$ = 294 Hz, **3b**). In the ^1H NMR spectra, the hydrogens of the CH_2 group of dppm appear as pseudo triplet resonances at δ 3.67 ppm ($^3J_{PtH}$ = 26.1 Hz, $^2J_{PH}$ = 10.6 Hz, **3a**), δ 2.94 ppm ($^3J_{PtH}$ = 21.8 Hz, $^2J_{PH}$ = 9.8 Hz, **3b**), and 4.15 ppm ($^2J_{PH}$ = 9.2 Hz, **3c**) with a small downfield shift from the equivalent resonances in **2a** (δ 3.42 ppm, $^3J_{PtH}$ = 25.3 Hz, $^2J_{PH}$ = 8.7 Hz), **2b** (δ 2.58 ppm, $^3J_{PtH}$ = 19.0 Hz, $^2J_{PH}$ =

https://dx.doi.org/10.1021/acs.organomet.0c00594
Organometallics XXXX, XXX, XXX−XXX

Table 2. Tandem Reaction of *p*-Haloacetophenones and Boronic Acids[a]

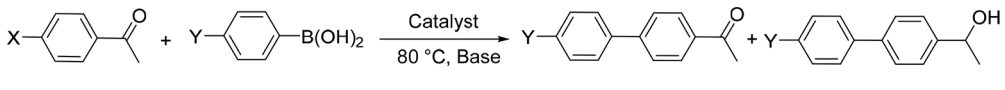

D E

						yield (%)[b]		
entry	catalyst	X	Y	base	time (h)	D	E	TON
1	**3c**	Br	H	Cs_2CO_3	5	-	98	490
2[c]	**3c**	Br	H	Cs_2CO_3	4	-	95	475
3[d]	**3c**	Br	H	Cs_2CO_3	5	30	-	150
4	**3c**	Br	H	NaO^{t}Bu	3	-	95	475
5	**3c**	Cl	H	Cs_2CO_3	5	10	86	480
6	**3c**	F	H	Cs_2CO_3	8	40	-	200
7	**3c**	F	H	NaO^{t}Bu	5	-	96	480
8	**3c**	Br	^{t}Bu	Cs_2CO_3	5	96	-	480
9	**3c**	Br	OMe	Cs_2CO_3	3	47	50	485
10	**3c**	Br	CF_3	Cs_2CO_3	5	-	95	475
11[e]	**3c**	Br	3,4,5-F	Cs_2CO_3	5	-	92	460
12	**3c**	F	^{t}Bu	NaO^{t}Bu	5	-	75	375
13	**3c**	F	CF_3	NaO^{t}Bu	5	-	83	415
14	**2c**	Br	H	Cs_2CO_3	20	18	10	140
15	**1**	Br	H	Cs_2CO_3	20	-	-	-
16	**3a**	Br	H	Cs_2CO_3	20	-	-	-
17	**3b**	Br	H	Cs_2CO_3	20	-	-	-
18	**1** + **2c**	Br	H	Cs_2CO_3	20	10	30	150

[a]Reaction conditions unless specified otherwise: *p*-haloacetophenone (1 mmol), $ArB(OH)_2$ (2 mmol), catalyst (2 mol %), base (3 mmol), EtOH (3 mL), 80 °C. [b]Isolated yields after preparatory thin-layer chromatography. [c]^{i}PrOH solvent. [d]EtOH;THF 2:1. [e]This boronic acid has three fluorine substituents.

Table 3. Catalytic Condensation of Nitrobenzenes and Benzyl Alcohols[a]

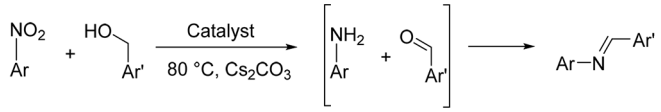

Entry	Catalyst	Ar-NO_2	Ar'CH_2OH	Product	Yield (%)[b]	TON
1	**1**	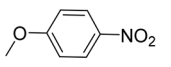	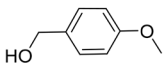	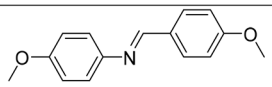	35	175
2	**2c**	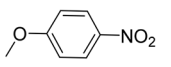	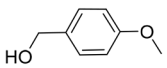	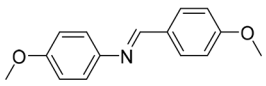	Trace	-
3	**3c**	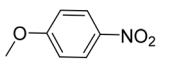	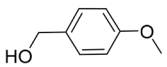	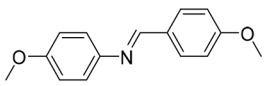	95	475
4	**3c**	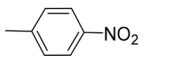	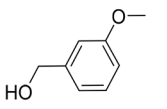	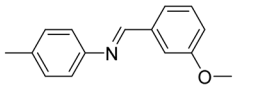	90	450
5	**3c**	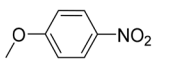	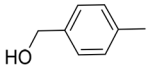	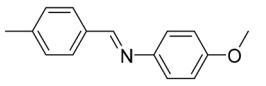	93	465
6	**3c**	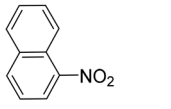	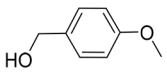	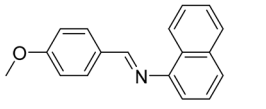	93	465

[a]Reaction conditions: nitrobenzene (1 mmol), benzyl alcohol (5 mmol) used as solvent and reagent, Cs_2CO_3 (3 mmol), catalyst (2 mol %) at 80 °C after 8 h. [b]Isolated yields after preparatory thin-layer chromatography.

https://dx.doi.org/10.1021/acs.organomet.0c00594
Organometallics XXXX, XXX, XXX−XXX

9.0 Hz), and **2c** (3.22 ppm, $^{2}J_{PH}$ = 9.5 Hz). The signals for methyl groups on the Cp* ligand (a singlet at δ 1.62 ppm for **3a,b** and a singlet at δ 1.74 ppm for **3c**), the methyl group coordinated to the platinum center in **3a** (a doublet at δ 0.94 ppm, $^{2}J_{PtH}$ = 77.8 Hz, $^{3}J_{PH}$ = 7.0 Hz), the methyl group of the *p*-MeC_6H_4 ligand in **3b** (a singlet at δ 1.99 ppm) and methyl groups coordinated to the TSC ligand (a doublet at δ 2.94 ppm with $^{3}J_{HH}$ = 4.9 Hz and a singlet at δ = 2.73 ppm) were assigned. Also, other characteristic resonances for ppy, Obpy, and TSC moieties are clearly distinguishable at the appropriate region.

The HR ESI-MS spectra of CH_3CN solution of **3a−c**, in positive mode, displayed an intense peak at m/z 776.2 (exact mass 776.2, Figure S1), which corresponds to the Rh fragment $[\{Cp^*Rh(ppy)(\kappa^1\text{-dppm})\}]^+$. This observation indicates that these heterobimetallic complexes perhaps are labile in the gas phase and undergo dissociation via rupture of the Pt−P or Pd−P bonds. According to the mass data, the observed peak can be reproduced by the reaction of **1** with the dppm ligand in 1:1 molar ratio and leads to the formation of the complex $[\{Cp^*Rh(ppy)(\kappa^1\text{-dppm})\}PF_6]$ (**4**) (see Scheme 2). This complex was readily characterized by NMR spectroscopy. In the $^{31}P\{^{1}H\}$ NMR spectrum of **4** (Figure 3), a doublet of doublets at δ 31.9 ppm with $^{1}J_{RhP^1}$ = 148 Hz and $^{2}J_{P^1P^2}$ = 54 Hz and a doublet at δ −29.3 ppm with $^{2}J_{P^1P^2}$ = 54 Hz are assigned for phosphorus atoms. A septet signal at δ −144.1 ppm with $^{1}J_{P^3F}$ = 713 Hz is attributed to PF_6. The ^{1}H NMR spectrum of **4** displays that the hydrogens of the CH_2 group of dppm have a diastereotopic feature. Those appeared as two clear doublet of doublets signals at δ 2.27 ppm with $^{1}J_{HH}$ = 14.6 Hz and $^{2}J_{PH}$ = 10.2 Hz and at δ 2.08 ppm with $^{1}J_{HH}$ = 14.6 Hz and $^{2}J_{PH}$ = 8.6 Hz. The methyl groups on the Cp* ligand are observed as a singlet signal at δ 1.43 ppm. Other characteristic peaks for the phenyl groups of dppm and ppy ligands appeared in the aromatic region.

Several attempts to obtain suitable single crystals of the heterobimetallic complexes for X-ray analysis were not successful. Therefore, to gain further insight into the structure of the heterobimetallic complexes, DFT calculations were used to optimize the geometry of **3c**. The structure of **1** was optimized (shown in Figure S2), and the selected geometrical parameters are presented in Table S2. The computed structural details are in good agreement with experimental parameters, showing that the B3LYP/LANL2DZ/6-31G(d) method is a reasonable compromise between accuracy and CPU time of calculations, and therefore we used it for the structural prediction of the new complex **3c**. The optimized structure of **3c** (Figure 4), the corresponding geometrical parameters (Table S2), charge distributions (Table S3), frontier orbitals (Figures S3 and S4 and Table S4), and overlaid experimental and calculated (TD-DFT) UV−vis absorption spectra (Figure S5 and Table S5) are collected in the Supporting Information. Also, comparative HOMO−LUMO gap diagrams of complexes **1**, **2c**, and **3c** are presented in Figures S6 and S7. In the simulated structure of **3c**, the coordination geometry of the rhodium center has a piano-stool feature which is similar to those observed in related complexes, such as **1**. The Cp* ring occupies three facial positions in the Rh environment by revealing the regular η^5 coordination mode. The palladium environment in **3c** is approximately square planar with the Pd(TSC) moiety, which is similar to the case for other Pd complexes.[53] The distance between the two phosphorus atoms in the dppm ligand is 3.175 Å, and a metal−metal bond is not found (the distance is 6.460 Å between Rh and Pd).

Catalytic Studies. On the basis of our previous experiences on the application of mono-[64−71] or heterobimetallic[72] complexes in catalytic reactions, the Rh^{III}−Pt (**3a,b**) and Rh^{III}−Pd^{II} (**3c**) complexes were applied in three different tandem reactions.

Transfer Hydrogenation (TH) and Dehalogenation (DH) Reactions. The catalytic activity of the synthesized mono- and heterobimetallic complexes were examined for TH/DH of different *p*-haloacetophenones. The three potential products **A**−**C** (see Table 1) are expected, depending on the relative rates of TH versus DH.[41] TH/DH reactions were performed under mildly basic conditions in the presence of Cs_2CO_3 in EtOH solvent as a source of hydrogen transfer at 90 °C. The mononuclear complexes alone show activity with Pd complex **2c** favoring DH and Rh complex **1** TH, but neither metal is as active as the heterobimetallic catalyst **3c**. Furthermore, the physical mixture of **1** and **2c** improves the selectivity toward product **C** (TH/DH) but is still significantly less effective than **3c**. This result supports cooperativity in the heterobimetallic catalyst.[37,41,42]

It is not surprising that Pd **2c** shows DH more than TH, favoring product **A** irrespective of the base or the alcohol hydrogen source (Table 1, entries 1−5). The Rh complex **1** is more effective toward ketone TH, and product **B** is favored (Table 1, entries 6−10). As would be expected, the physical mixture of **1** and **2c** produces **C** (TH/DH product) but only in a 53% yield after 24 h (Table 1, entry 11). This is in sharp contrast to a 96% yield of product **C** in 8 h with the bimetallic Rh−Pd catalyst **3c** (entry 14). Interestingly, the bimetallic catalyst shows the best performance with a milder base and EtOH in comparison to ^{i}PrOH. Also, our study extended to checking the catalytic activity of **4** (entries 17 and 18), which showed higher activity in comparison to **1** in the TH reaction. Perhaps this may be related to the presence of a phosphine ligand in its structure. The Rh−Pt bimetallic catalysts **3a,b** exhibit unremarkable activity with very modest yields, which could be attributed to Rh alone (entries 19−25) on the basis of the product selectivity for **B**. According to the obtained results, **3c** was more active than **3a,b** (Table 1) in this tandem reaction.

The time resolution of the tandem reaction in the presence of **3c** as the catalyst and *p*-bromoacetophenone is shown in Figure 5, which provided more insight about the progress of the TH/DH catalytic process. The reactant *p*-bromoacetophenone was consumed essentially during 2 h, and **A** and **B** in that time peaked at ca. 70% and 20%, respectively. Over the subsequent 5 h, both **A** and **B** decreased and the TH/DH final product **C** increased. This is consistent with a reactant → **A**/**B** → **C** sequential process. On the basis of the relative accumulation of **A** versus **B**, DH is somewhat faster than TH.

The stability of **3c** was also investigated under the optimized conditions; the solution NMR spectra did not show any decomposition even after 5 h. Only after 48 h could a small amount of Pd black or unidentified decomposition products (less than 5%) be observed. This experiment confirmed that **3c** was stable under the reaction conditions. Additionally, the crystallinity of **3c** was investigated by powder X-ray diffraction (PXRD), as shown in Figure S8. This complex revealed a peak at 2θ = 40.20° corresponding to Pd(111) and a peak at 2θ = 41.15° assigned to Rh(111). The PXRD spectrum of recovered **3c** after TH/DH reactions confirmed that its crystallinity was retained.

The results obtained for the TH/DH tandem reaction suggest two consecutive reaction cycles to promote a tandem process, as shown in Scheme 3. The DH of aryl halide and hydrogenation of

https://dx.doi.org/10.1021/acs.organomet.0c00594
Organometallics XXXX, XXX, XXX−XXX

Table 4. Comparison of Catalytic Activities of 3c with Previously Reported Catalysts in the Three Studied Tandem Reactions

Entry	Catalyst	Reaction	Time (h)	Temp. (°C)	Base	Solvent	Yield (%)	Ref.
1	**3c**	TH/DH	8	80 °C	Cs_2CO_3	EtOH	96	This work
2	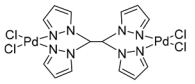	TH/DH	8	80 °C	KO′Bu	^{i}PrOH	98	74
3	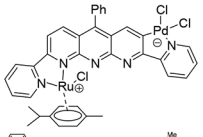	TH/DH	20	80 °C	NaOH	^{i}PrOH	100	41
4	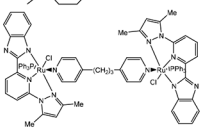	TH[a]	1 min	82 °C	^{i}PrOK	^{i}PrOH	99	79
5	$Pd_{36}Co_{64}$@HCCs	TH	10	90 °C	KOH	^{i}PrOH	99	80
6	$Pd(dba)_2$, SIMes.HCl[b]	DH	1	100 °C	KOMe	Dioxane	100	75
7	$In(OAc)_3$, $PhSiH_3$[c]	DH	24		K_2CO_3	THF	95	81
8	**3c**	TH/Suzuki coupling	5	80 °C	Cs_2CO_3	EtOH	98	This work
9	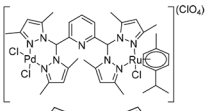	TH/Suzuki coupling	2.5	80 °C	KO′Bu	^{i}PrOH	97	82
10	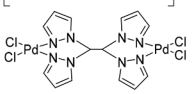	TH/Suzuki coupling	20	80 °C	KO′Bu	^{i}PrOH	92	74
11	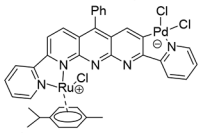	TH/Suzuki coupling	20	80 °C	NaOH	^{i}PrOH	97	41
12	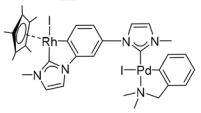	TH/Suzuki coupling	20	100 °C	Cs_2CO_3	^{i}PrOH	82	37
13	**3c**	Schiff base	8	80 °C	Cs_2CO_3		95	This work
14	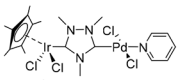	Schiff base	12	110 °C	Cs_2CO_3		70	35
15	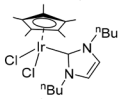	Schiff base[d]	7	110 °C	AgTOF	Toluene-d_8	95	83
16	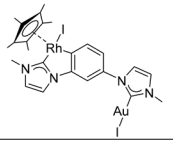	Schiff base	20	100 °C	Cs_2CO_3		34	42

[a]Under an inert atmosphere (N_2), [b]Bromotoluene. [c]Iodobenzamide, [d]benzyl alcohol, aniline.

carbonyl occur over Pd (cycle I)[73−75] and Rh of **3c** (cycle II),[45,76,77] respectively, leading to the tandem process. In the DH cycle, the Pd center in **3c** activates the Ar−X bond through an oxidative addition process.[73] In the next step, halide was replaced by an ethoxide anion (formed by the reaction of EtOH and Cs_2CO_3) in the coordination sphere of the Pd center. This process is followed by a β-hydrogen elimination[78] of coordinated ethoxide (yielding formaldehyde) and a reductive elimination step (producing product **A** in Scheme 3) that regenerated the initial Pd species. In the second cycle, the Rh center of **3c**, in the presence of Cs_2CO_3, reacts with EtOH to give an ethoxy−Rh fragment, which results in a β-hydrogen elimination, producing an Rh−H bond. This Rh hydride center reacts with compound **A** (obtained from cycle I) to produce **C**, regenerating the active catalyst. A series of calculations have been performed in order to propose the possible structure for intermediates shown in Scheme 3, in which Cp* and the Ph group of the dppm ligand are replaced by Cp and Me, respectively, due to computational cost. The lowest energy structures of the complexes **F**−**H** and **J**−**L** and their relative energies to **3c**, as calculated by density functional theory (DFT), are shown in Figure 6.

TH/Suzuki−Miyaura Cross-Coupling Reactions. The heterobimetallic complex **3c**, as a catalyst, was applied to another tandem reaction (TH/Suzuki−Miyaura cross coupling).[37] For this purpose, different *p*-haloacetophenones and boronic acids in

https://dx.doi.org/10.1021/acs.organomet.0c00594
Organometallics XXXX, XXX, XXX−XXX

the presence of heterobimetallic complexes **3a**−**c** (or the monometallic complexes **1** and **2c**, to compare their catalytic activity) and different bases and alcohol solvents were examined to find the optimal conditions (see Table 2). The reaction of phenylboronic acid and *p*-bromoacetophenone in the presence of Cs_2CO_3 and **3c** in EtOH (entry 1) led to a tandem reaction and product **E** in 98% yield. When the solvent was changed to ^{i}PrOH, the rate of the reaction was slightly faster and the yield was comparable to that for EtOH (entry 2). In the mixed solvent system EtOH:THF (2:1), only compound **D** was observed in low yield (entry 3). Interestingly, *p*-fluoroacetophenone converted to **E** only in the presence of the stronger base NaO^{t}Bu (entry 7), while in the presence of Cs_2CO_3 only **D** in low yield was obtained (entry 6). By a change in substituents on the boronic acids, **D** (entries 8 and 9) and **E** (entries 9−13) were obtained. These results indicated that electron-withdrawing groups on the boronic acids were more effective than electron-donating substituents (except for entry 13 in the presence of NaO^{t}Bu). The use of the monometallic Pd complex **2c** gave low yields even after 20 h (entry 14). No TH/Suzuki−Miyaura cross coupling reaction was observed in the presence of **1** (entry 15) and heterobimetallic complexes **3a**,**b** (entries 16 and 17). A slight synergic effect was observed in the mixture of **1** + **2c** (entry 18), and it led to the formation of **D** (10%) and **E** (30%). The data suggest a mechanism for the tandem reaction, catalyzed by **3c**, in two cycles as shown in Scheme S1. Cycle I (Pd center) involves a C−C cross-coupling reaction, and the reduction of carbonyl to alcohol takes place in cycle II (Rh center).

Condensation of Nitroarenes and Primary Alcohols. In general, Schiff base production proceeds in three steps: (1) preparation of an aldehyde through the oxidation of benzyl alcohol, (2) amine synthesis by reduction of a nitroarene, and (3) condensation reaction between the amine and the aldehyde to afford the corresponding Schiff base.[42] To obtain suitable conditions for the condensation reaction, reactions were carried out in the presence of nitroarene, benzyl alcohols, and catalyst. Entries 1−3 indicate different catalytic activities for **1**, **2c**, and **3c** under the same conditions. On the basis of these results, **3c** was selected as the best performer (on the basis of on reaction time and yield), while **1** and **2c** were inferior, not reaching completion even after 24 h. Obviously, these data exhibited a notable result for nitro reduction in the presence of **1** by metal hydride transformation and oxidation of the alcohol to give a related Schiff base (35%). From another point of view, **2c** was not appropriate for alcohol oxidation to aldehyde and transfer hydrogenation for reducing nitrobenzene to aniline, and it displayed a trace amount of *N*-benzylideneaniline. According to this result, a pathway can be proposed for this tandem reaction in two steps by using **3c** as a catalyst. The Rh center in **3c** can dehydrogenate the alcohol, while the Pd center in **3c** facilitates nitrobenzene reduction by using the released hydrogen (from alcohol dehydrogenation, see Scheme S2). Therefore, the heterobimetallic complex **3c** was applied as a homogeneous catalyst in the coupling between various benzyl alcohols and nitrobenzenes to prepare imines (Schiff bases). The catalytic reaction was performed with 2 mol % of catalyst (**3c**) loading in the presence of 5 mmol of benzyl alcohol (which was used as both solvent and hydrogen donor), 1 mmol of nitrobenzenes, and Cs_2CO_3 (base) at 80 °C. Under these conditions various Schiff base compounds were prepared cleanly via the tandem reaction, and the results are collected in Table 3. In this process, 2 equiv of benzaldehyde in all entries was observed for every 1 equiv of an imine product.

CONCLUSIONS

The present investigation summarizes the synthesis of a new category of heterobimetallic complexes bearing Rh^{III}−Pt^{II} and Rh^{III}−Pd^{II}, via dppm as the bridging ligand. The isolated complexes have been characterized by various spectroscopic techniques. The enhanced catalytic activities of these air-stable complexes have been applied for three different tandem reactions: TH/DH, TH/Suzuki−Miyaura coupling, and coupling of nitrobenzenes with benzylic alcohols for imine synthesis. We used EtOH (instead of the previously reported ^{i}PrOH)[37,41] as an uncommon hydrogen source and solvent.[46,47] The scope of these tandem processes is very broad, covering electron-rich and electron-deficient *p*-haloacetophenones or nitroarenes. The Rh^{III}−Pd^{II} complex **3c** shows higher activity in comparison the mono- and heterobimetallic complexes reported in this work. Consequently, the cooperation between the Rh and Pd metal centers provides an efficient catalyst.[37,41,42] A proposed mechanism pathway for the TH/DH tandem reaction displays the role of each metal center in this process. It suggests that the DH of aryl halide and hydrogenation of carbonyl occurs with the assistance of Pd (cycle I) and Rh centers of **3c** (cycle II), respectively, leading to the tandem process. This investigation opens a new avenue for designing efficient heterobimetallic systems for various organic transformations.

The heterobimetallic complex Rh^{III}−Pd^{II} reported here has better efficiency, has higher rates, requires lower temperatures, and uses a weaker base (Cs_2CO_3) in comparison with other reported catalysts (see Table 4). As noted, the key point in this study is using EtOH as a solvent with low toxicity in comparison to ^{i}PrOH as a common solvent for tandem reactions.

ASSOCIATED CONTENT

Supporting Information

The Supporting Information is available free of charge at https://pubs.acs.org/doi/10.1021/acs.organomet.0c00594.

NMR spectra of organic compounds, crystallographic and computational details (PDF)

Cartesian coordinates for the calculated structures (XYZ)

Accession Codes

CCDC 1997183 contains the supplementary crystallographic data for this paper. These data can be obtained free of charge via www.ccdc.cam.ac.uk/data_request/cif, or by emailing data_request@ccdc.cam.ac.uk, or by contacting The Cambridge Crystallographic Data Centre, 12 Union Road, Cambridge CB2 1EZ, UK; fax: +44 1223 336033.

AUTHOR INFORMATION

Corresponding Authors

S. Masoud Nabavizadeh − *Professor Rashidi Laboratory of Organometallic Chemistry, Department of Chemistry, College of Sciences, Shiraz University, Shiraz 71467-13565, Iran;* orcid.org/0000-0003-3976-7869; Email: nabavizadeh@shirazu.ac.ir

Hamid R. Shahsavari − *Department of Chemistry, Institute for Advanced Studies in Basic Sciences (IASBS), Zanjan 45137-66731, Iran;* orcid.org/0000-0002-2579-2185; Email: shahsavari@iasbs.ac.ir

Mahdi M. Abu-Omar − *Department of Chemistry and Biochemistry, University of California, Santa Barbara, California 93106, United States;* orcid.org/0000-0002-4412-1985; Email: abuomar@chem.ucsb.edu

https://dx.doi.org/10.1021/acs.organomet.0c00594
Organometallics XXXX, XXX, XXX−XXX

Authors

Zeinab Mandegani − *Professor Rashidi Laboratory of Organometallic Chemistry, Department of Chemistry, College of Sciences, Shiraz University, Shiraz 71467-13565, Iran*

Asma Nahaei − *Professor Rashidi Laboratory of Organometallic Chemistry, Department of Chemistry, College of Sciences, Shiraz University, Shiraz 71467-13565, Iran*

Mahshid Nikravesh − *Department of Chemistry, Institute for Advanced Studies in Basic Sciences (IASBS), Zanjan 45137-66731, Iran*

Complete contact information is available at: https://pubs.acs.org/10.1021/acs.organomet.0c00594

Author Contributions

‖Z.M. and A.N. contributed equally to this work.

Notes

The authors declare no competing financial interest.

■ ACKNOWLEDGMENTS

This work was supported by Shiraz University, the Institute for Advanced Studies in Basic Sciences (IASBS) Research Council (G2020IASBS32629), the Iran National Science Foundation (Grant No. 96008511), and the Department of Chemistry and Biochemistry at UCSB.

■ REFERENCES

(1) Li, Z.; Ji, S.; Liu, Y.; Cao, X.; Tian, S.; Chen, Y.; Niu, Z.; Li, Y. Well-Defined Materials for Heterogeneous Catalysis: From Nanoparticles to Isolated Single-Atom Sites. *Chem. Rev.* **2020**, *120*, 623−682.

(2) Hutchings, G.; Davidson, M.; Catlow, R.; Hardacre, C.; Turner, N.; Collier, P. *Modern Developments in Catalysis*; World Scientific: 2017.

(3) Anderson, J. A.; García, M. F. *Supported Metals in Catalysis*; World Scientific: 2011.

(4) Lorion, M. M.; Maindan, K.; Kapdi, A. R.; Ackermann, L. Heteromultimetallic catalysis for sustainable organic syntheses. *Chem. Soc. Rev.* **2017**, *46*, 7399−7420.

(5) Mata, J. A.; Hahn, F. E.; Peris, E. Heterometallic complexes, tandem catalysis and catalytic cooperativity. *Chem. Sci.* **2014**, *5*, 1723−1732.

(6) Buchwalter, P.; Rosé, J.; Braunstein, P. Multimetallic Catalysis Based on Heterometallic Complexes and Clusters. *Chem. Rev.* **2015**, *115*, 28−126.

(7) Bratko, I.; Gómez, M. Polymetallic complexes linked to a single-frame ligand: cooperative effects in catalysis. *Dalton Trans.* **2013**, *42*, 10664−10681.

(8) van den Beuken, E. K.; Feringa, B. L. Bimetallic catalysis by late transition metal complexes. *Tetrahedron* **1998**, *54*, 12985−13011.

(9) Karunananda, M. K.; Vázquez, F. X.; Alp, E. E.; Bi, W.; Chattopadhyay, S.; Shibata, T.; Mankad, N. P. Experimental determination of redox cooperativity and electronic structures in catalytically active Cu−Fe and Zn−Fe heterobimetallic complexes. *Dalton Trans.* **2014**, *43*, 13661−13671.

(10) Karimi, B.; Barzegar, H.; Vali, H. Au-Pd bimetallic nanoparticles supported on a high nitrogen-rich ordered mesoporous carbon as an efficient catalyst for room temperature Ullmann coupling of aryl chlorides in aqueous media. *Chem. Commun.* **2018**, *54*, 7155−7158.

(11) Ghosh, P.; Ding, S.; Chupik, R. B.; Quiroz, M.; Hsieh, C.-H.; Bhuvanesh, N.; Hall, M. B.; Darensbourg, M. Y. A matrix of heterobimetallic complexes for interrogation of hydrogen evolution reaction electrocatalysts. *Chem. Sci.* **2017**, *8*, 8291−8300.

(12) Tang, H.; Hall, M. B. Biomimetics of [NiFe]-Hydrogenase: Nickel- or Iron-Centered Proton Reduction Catalysis? *J. Am. Chem. Soc.* **2017**, *139*, 18065−18070.

(13) Pezük, L. G.; Şen, B.; Hahn, F. E.; Türkmen, H. Heterobimetallic Complexes Bridged by Imidazol{[4,5-f][1,10]-phenanthrolin}-2-ylidene: Synthesis and Catalytic Activity in Tandem Reactions. *Organometallics* **2019**, *38*, 593−601.

(14) Fong, H.; Moret, M.-E.; Lee, Y.; Peters, J. C. Heterolytic H_2 Cleavage and Catalytic Hydrogenation by an Iron Metallaboratrane. *Organometallics* **2013**, *32*, 3053−3062.

(15) Gramigna, K. M.; Dickie, D. A.; Foxman, B. M.; Thomas, C. M. Cooperative H_2 Activation across a Metal−Metal Multiple Bond and Hydrogenation Reactions Catalyzed by a Zr/Co Heterobimetallic Complex. *ACS Catal.* **2019**, *9*, 3153−3164.

(16) Ferreira, R. B.; Murray, L. J. Cyclophanes as Platforms for Reactive Multimetallic Complexes. *Acc. Chem. Res.* **2019**, *52*, 447−455.

(17) Anderson, J. S.; Rittle, J.; Peters, J. C. Catalytic conversion of nitrogen to ammonia by an iron model complex. *Nature* **2013**, *501*, 84−87.

(18) Chu, X.; Jin, J.; Ming, B.; Pang, M.; Yu, X.; Tung, C.-H.; Wang, W. Bimetallic nickel−cobalt hydrides in H2 activation and catalytic proton reduction. *Chem. Sci.* **2019**, *10*, 761−767.

(19) Charles, R. M., III; Yokley, T. W.; Schley, N. D.; DeYonker, N. J.; Brewster, T. P. Hydrogen Activation and Hydrogenolysis Facilitated By Late-Transition-Metal−Aluminum Heterobimetallic Complexes. *Inorg. Chem.* **2019**, *58*, 12635−12645.

(20) Pye, D. R.; Mankad, N. P. Bimetallic catalysis for C−C and C−X coupling reactions. *Chem. Sci.* **2017**, *8*, 1705−1718.

(21) Fu, J.; Huo, X.; Li, B.; Zhang, W. Cooperative bimetallic catalysis in asymmetric allylic substitution. *Org. Biomol. Chem.* **2017**, *15*, 9747−9759.

(22) Luengo, A.; Fernández-Moreira, V.; Marzo, I.; Gimeno, M. C. Trackable Metallodrugs Combining Luminescent Re(I) and Bioactive Au(I) Fragments. *Inorg. Chem.* **2017**, *56*, 15159−15170.

(23) Fernández-Moreira, V.; Gimeno, M. C. Heterobimetallic Complexes for Theranostic Applications. *Chem. - Eur. J.* **2018**, *24*, 3345−3353.

(24) Curado, N.; Contel, M., Heterometallic Complexes as Anticancer Agents. In *Metal-based Anticancer Agents*; The Royal Society of Chemistry: 2019; pp 143−168.

(25) Fernández-Moreira, V.; Marzo, I.; Gimeno, M. C. Luminescent Re(I) and Re(I)/Au(I) complexes as cooperative partners in cell imaging and cancer therapy. *Chem. Sci.* **2014**, *5*, 4434−4446.

(26) Wenzel, M.; Bigaeva, E.; Richard, P.; Le Gendre, P.; Picquet, M.; Casini, A.; Bodio, E. New heteronuclear gold(I)−platinum(II) complexes with cytotoxic properties: Are two metals better than one? *J. Inorg. Biochem.* **2014**, *141*, 10−16.

(27) Bertrand, B.; Citta, A.; Franken, I. L.; Picquet, M.; Folda, A.; Scalcon, V.; Rigobello, M. P.; Le Gendre, P.; Casini, A.; Bodio, E. Gold(I) NHC-based homo- and heterobimetallic complexes: synthesis, characterization and evaluation as potential anticancer agents. *J. Biol. Inorg. Chem.* **2015**, *20*, 1005−1020.

(28) Puddephatt, R. J. Chemistry of bis(diphenylphosphino)methane. *Chem. Soc. Rev.* **1983**, *12*, 99−127.

(29) Shahsavari, H. R.; Giménez, N.; Lalinde, E.; Moreno, M. T.; Fereidoonnezhad, M.; Babadi Aghakhanpour, R.; Khatami, M.; Kalantari, F.; Jamshidi, Z.; Mohammadpour, M. Heterobimetallic Pt^{II}-Au^{I} Complexes Comprising Unsymmetrical 1,1-Bis(diphenylphosphanyl)methane Bridges: Synthesis, Photophysical, and Cytotoxic Studies. *Eur. J. Inorg. Chem.* **2019**, 1360−1373.

(30) Nazari, M.; Shahsavari, H. R. Strong red emissions induced by Pt−Pt interactions in binuclear cycloplatinated(II) complexes containing bridging diphosphines. *Appl. Organomet. Chem.* **2019**, *33*, e5020.

(31) Nabavizadeh, S. M.; Golbon Haghighi, M.; Esmaeilbeig, A. R.; Raoof, F.; Mandegani, Z.; Jamali, S.; Rashidi, M.; Puddephatt, R. J. Assembly of Symmetrical or Unsymmetrical Cyclometalated Organoplatinum Complexes through a Bridging Diphosphine Ligand. *Organometallics* **2010**, *29*, 4893−4899.

(32) Aghakhanpour, R. B.; Nabavizadeh, S. M.; Rashidi, M.; Kubicki, M. Luminescence properties of some monomeric and dimeric cycloplatinated(II) complexes containing biphosphine ligands. *Dalton Trans.* **2015**, *44*, 15829−15842.

https://dx.doi.org/10.1021/acs.organomet.0c00594
Organometallics XXXX, XXX, XXX−XXX

(33) Sangari, M. S.; Haghighi, M. G.; Nabavizadeh, S. M.; Kubicki, M.; Rashidi, M. Photophysical study on unsymmetrical binuclear cycloplatinated(II) complexes. *New J. Chem.* **2017**, *41*, 13293−13302.
(34) Lohr, T. L.; Marks, T. J. Orthogonal tandem catalysis. *Nat. Chem.* **2015**, *7*, 477−482.
(35) Zanardi, A.; Mata, J. A.; Peris, E. One-Pot Preparation of Imines from Nitroarenes by a Tandem Process with an Ir−Pd Heterodimetallic Catalyst. *Chem. - Eur. J.* **2010**, *16*, 10502−10506.
(36) Chen, X.; Han, S.; Yin, D.; Liang, C. Intermetallic Ni_2Si/SiCN as a highly efficient catalyst for the one-pot tandem synthesis of imines and secondary amines. *Inorg. Chem. Front.* **2020**, *7*, 82−90.
(37) Böhmer, M.; Guisado-Barrios, G.; Kampert, F.; Roelfes, F.; Tan, T. T. Y.; Peris, E.; Hahn, F. E. Synthesis and Catalytic Applications of Heterobimetallic Carbene Complexes Obtained via Sequential Metalation of Two Bisazolium Salts. *Organometallics* **2019**, *38*, 2120−2131.
(38) Slaney, M. E.; Ferguson, M. J.; McDonald, R.; Cowie, M. Tandem C−F and C−H Bond Activation in Fluoroolefins Promoted by a Bis(diethylphosphino)methane-Bridged Diiridium Complex: Role of Water in the Activation Processes. *Organometallics* **2012**, *31*, 1384−1396.
(39) Ahrens, T.; Kohlmann, J.; Ahrens, M.; Braun, T. Functionalization of Fluorinated Molecules by Transition-Metal-Mediated C−F Bond Activation To Access Fluorinated Building Blocks. *Chem. Rev.* **2015**, *115*, 931−972.
(40) Slaney, M. E.; Anderson, D. J.; Ferguson, M. J.; McDonald, R.; Cowie, M. Bis(diethylphosphino)methane As a Bridging Ligand in Complexes of Ir_2, Rh_2, and IrRh: Geminal C−H Activation of α-Olefins. *Organometallics* **2012**, *31*, 2286−2301.
(41) Lin, S.-C. A.; Liu, Y.-H.; Peng, S.-M.; Liu, S.-T. Hetero-Bimetallic Complexes Based on an Anthyridine Ligand Preparation and Catalytic Activity. *Organometallics* **2020**, *39*, 123−131.
(42) Böhmer, M.; Kampert, F.; Tan, T. T. Y.; Guisado-Barrios, G.; Peris, E.; Hahn, F. E. Ir^{III}/Au^{I} and Rh^{III}/Au^{I} Heterobimetallic Complexes as Catalysts for the Coupling of Nitrobenzene and Benzylic Alcohol. *Organometallics* **2018**, *37*, 4092−4099.
(43) Panda, B.; Sarkar, T. K. Gold and palladium combined for the Sonogashira-type cross-coupling of arenediazonium salts. *Chem. Commun.* **2010**, *46*, 3131−3133.
(44) Seitz, S. C.; Rominger, F.; Straub, B. F. Stepwise Deprotonation of a Thiol-Functionalized Bis(1,2,4-triazolium) Salt as a Selective Route to Heterometallic NHC Complexes. *Organometallics* **2013**, *32*, 2427−2434.
(45) Zweifel, T.; Naubron, J.-V.; Büttner, T.; Ott, T.; Grützmacher, H. Ethanol as Hydrogen Donor: Highly Efficient Transfer Hydrogenations with Rhodium(I) Amides. *Angew. Chem., Int. Ed.* **2008**, *47*, 3245−3249.
(46) Weingart, P.; Thiel, W. R. Applying Le Chatelier's Principle for a Highly Efficient Catalytic Transfer Hydrogenation with Ethanol as the Hydrogen Source. *ChemCatChem* **2018**, *10*, 4844−4848.
(47) Wang, Y.; Huang, Z.; Leng, X.; Zhu, H.; Liu, G.; Huang, Z. Transfer Hydrogenation of Alkenes Using Ethanol Catalyzed by a NCP Pincer Iridium Complex: Scope and Mechanism. *J. Am. Chem. Soc.* **2018**, *140*, 4417−4429.
(48) Wang, C.; Gong, S.; Liang, Z.; Sun, Y.; Cheng, R.; Yang, B.; Liu, Y.; Yang, J.; Sun, F. Ligand-Promoted Iridium-Catalyzed Transfer Hydrogenation of Terminal Alkynes with Ethanol and Its Application. *ACS Omega* **2019**, *4*, 16045−16051.
(49) Shahsavari, H. R.; Babadi Aghakhanpour, R.; Nikravesh, M.; Ozdemir, J.; Golbon Haghighi, M.; Notash, B.; Beyzavi, M. H. Highly Emissive Cycloplatinated(II) Complexes Obtained by the Chloride Abstraction from the Complex $[Pt(ppy)(PPh_3)(Cl)]$: Employing Various Silver Salts. *Organometallics* **2018**, *37*, 2890−2900.
(50) Li, L.; Brennessel, W. W.; Jones, W. D. An Efficient Low-Temperature Route to Polycyclic Isoquinoline Salt Synthesis via C−H Activation with $[Cp^*MCl_2]_2$ (M = Rh, Ir). *J. Am. Chem. Soc.* **2008**, *130*, 12414−12419.
(51) Hu, Y.; Li, L.; Shaw, A. P.; Norton, J. R.; Sattler, W.; Rong, Y. Synthesis, Electrochemistry, and Reactivity of New Iridium(III) and Rhodium(III) Hydrides. *Organometallics* **2012**, *31*, 5058−5064.
(52) Fereidoonnezhad, M.; Niazi, M.; Shahmohammadi Beni, M.; Mohammadi, S.; Faghih, Z.; Faghih, Z.; Shahsavari, H. R. Synthesis, Biological Evaluation, and Molecular Docking Studies on the DNA Binding Interactions of Platinum(II) Rollover Complexes Containing Phosphorus Donor Ligands. *ChemMedChem* **2017**, *12*, 456−465.
(53) Martínez, J.; Adrio, L. A.; Antelo, J. M.; Pereira, M. T.; Fernández, J. J.; Vila, J. M. New thiosemicarbazone palladacycles with chelating bis(diphenylphosphino)methane. *Polyhedron* **2006**, *25*, 2848−2858.
(54) Frisch, M. J.; Trucks, G. W.; Schlegel, H. B.; Scuseria, G. E.; Robb, M. A.; Cheeseman, J. R.; Scalmani, G.; Barone, V.; Petersson, G. A.; Nakatsuji, H.; Li, X.; Caricato, M.; Marenich, A. V.; Bloino, J.; Janesko, B. G.; Gomperts, R.; Mennucci, B.; Hratchian, H. P.; Ortiz, J. V.; Izmaylov, A. F.; Sonnenberg, J. L.; Williams; Ding, F.; Lipparini, F.; Egidi, F.; Goings, J.; Peng, B.; Petrone, A.; Henderson, T.; Ranasinghe, D.; Zakrzewski, V. G.; Gao, J.; Rega, N.; Zheng, G.; Liang, W.; Hada, M.; Ehara, M.; Toyota, K.; Fukuda, R.; Hasegawa, J.; Ishida, M.; Nakajima, T.; Honda, Y.; Kitao, O.; Nakai, H.; Vreven, T.; Throssell, K.; Montgomery, J. A., Jr.; Peralta, J. E.; Ogliaro, F.; Bearpark, M. J.; Heyd, J. J.; Brothers, E. N.; Kudin, K. N.; Staroverov, V. N.; Keith, T. A.; Kobayashi, R.; Normand, J.; Raghavachari, K.; Rendell, A. P.; Burant, J. C.; Iyengar, S. S.; Tomasi, J.; Cossi, M.; Millam, J. M.; Klene, M.; Adamo, C.; Cammi, R.; Ochterski, J. W.; Martin, R. L.; Morokuma, K.; Farkas, O.; Foresman, J. B.; Fox, D. J. *Gaussian 16,Rev. C.01*: Gaussian Inc.: Wallingford, CT, 2016.
(55) Wadt, W. R.; Hay, P. J. Ab initio effective core potentials for molecular calculations. Potentials for main group elements Na to Bi. *J. Chem. Phys.* **1985**, *82*, 284−298.
(56) Skripnikov, L. *Chemissian: software to analyze spectra, build density maps and molecular orbitals, Ver. 4*; 2016, .
(57) Sheldrick, G. *SADABS, Empirical Absorption Correction Program*; University of Göttingen: Göttingen, Germany, 1997.
(58) *SHELXTL PC, Ver. 6.12*; Bruker AXS Inc.: Madison, WI, 2005.
(59) Hopkins, J. A.; Lionetti, D.; Day, V. W.; Blakemore, J. D. Chemical and Electrochemical Properties of [Cp*Rh] Complexes Supported by a Hybrid Phosphine-Imine Ligand. *Organometallics* **2019**, *38*, 1300−1310.
(60) Camarena-Díaz, J. P.; Iglesias, A. L.; Chávez, D.; Aguirre, G.; Grotjahn, D. B.; Rheingold, A. L.; Parra-Hake, M.; Miranda-Soto, V. $Rh^{(III)}Cp^*$ and $Ir^{(III)}Cp^*$ Complexes of 1-[(4-Methyl)phenyl]-3-[(2-methyl-4′-R)imidazol-1-yl]triazenide (R = *t*-Bu or H): Synthesis, Structure, and Catalytic Activity. *Organometallics* **2019**, *38*, 844−851.
(61) Nabavizadeh, S. M.; Sepehrpour, H.; Kia, R.; Rheingold, A. L. Bis(diphenylphosphino)acetylene as bifunctional ligand in cycloplatinated complexes: Synthesis, characterization, crystal structures and mechanism of MeI oxidative addition. *J. Organomet. Chem.* **2013**, *745*−*746*, 148−157.
(62) Nabavizadeh, S. M.; Dadkhah Aseman, M.; Ghaffari, B.; Rashidi, M.; Hosseini, F. N.; Azimi, G. Kinetics and mechanism of oxidative addition of MeI to binuclear cycloplatinated complexes containing biphosphine bridges: Effects of ligands. *J. Organomet. Chem.* **2012**, *715*, 73−81.
(63) Jamali, S.; Nabavizadeh, S. M.; Rashidi, M. Binuclear Cyclometalated Organoplatinum Complexes Containing 1,1′-Bis(diphenylphosphino)ferrocene as Spacer Ligand: Kinetics and Mechanism of MeI Oxidative Addition. *Inorg. Chem.* **2008**, *47*, 5441−5452.
(64) Nabavizadeh, S. M.; Niroomand Hosseini, F.; Park, C.; Wu, G.; Abu-Omar, M. M. Discovery and mechanistic investigation of Pt-catalyzed oxidative homocoupling of benzene with $PhI(OAc)_2$. *Dalton Trans.* **2020**, *49*, 2477−2486.
(65) Mosleh, I.; Shahsavari, H. R.; Beitle, R.; Beyzavi, M. H. Recombinant Peptide Fusion Protein-templated Palladium Nanoparticles for Suzuki-Miyaura and Stille Coupling Reactions. *ChemCatChem* **2020**, *12*, 2942−2946.
(66) Zare Asadabadi, A.; Hoseini, S. J.; Bahrami, M.; Nabavizadeh, S. M. Catalytic applications of β-cyclodextrin/palladium nanoparticle thin film obtained from oil/water interface in the reduction of toxic

https://dx.doi.org/10.1021/acs.organomet.0c00594
Organometallics XXXX, XXX, XXX−XXX

nitrophenol compounds and the degradation of azo dyes. *New J. Chem.* **2019**, *43*, 6513−6522.
(67) Mandegani, Z.; Asadi, M.; Asadi, Z.; Mohajeri, A.; Iranpoor, N.; Omidvar, A. A nano tetraimine Pd(0) complex: synthesis, characterization, computational studies and catalytic applications in the Heck−Mizoroki reaction in water. *Green Chem.* **2015**, *17*, 3326−3337.
(68) Gholinejad, M.; Shahsavari, H. R. N,N′-bis(2-pyridinecarboxamide)-1,2-benzene palladium complex as a new efficient catalyst for Suzuki−Miyaura coupling reaction under phosphane free conditions. *Inorg. Chim. Acta* **2014**, *421*, 433−438.
(69) Gunasekara, T.; Kim, J.; Preston, A.; Steelman, D. K.; Medvedev, G. A.; Delgass, W. N.; Sydora, O. L.; Caruthers, J. M.; Abu-Omar, M. M. Mechanistic Insights into Chromium-Catalyzed Ethylene Trimerization. *ACS Catal.* **2018**, *8*, 6810−6819.
(70) Switzer, J. M.; Pletcher, P. D.; Steelman, D. K.; Kim, J.; Medvedev, G. A.; Abu-Omar, M. M.; Caruthers, J. M.; Delgass, W. N. Quantitative Modeling of the Temperature Dependence of the Kinetic Parameters for Zirconium Amine Bis(Phenolate) Catalysts for 1-Hexene Polymerization. *ACS Catal.* **2018**, *8*, 10407−10418.
(71) Pletcher, P. D.; Switzer, J. M.; Steelman, D. K.; Medvedev, G. A.; Delgass, W. N.; Caruthers, J. M.; Abu-Omar, M. M. Quantitative Comparative Kinetics of 1-Hexene Polymerization across Group IV Bis-Phenolate Catalysts. *ACS Catal.* **2016**, *6*, 5138−5145.
(72) Gholinejad, M.; Shahsavari, H. R.; Razeghi, M.; Niazi, M.; Hamed, F. 2-(diphenylphosphino)pyridine platinum(I) and palladium-(I) complex as an efficient binuclear catalyst for Suzuki-Miyaura coupling reaction in water under mild reaction conditions. *J. Organomet. Chem.* **2015**, *796*, 3−10.
(73) Navarro, O.; Kaur, H.; Mahjoor, P.; Nolan, S. P. Cross-Coupling and Dehalogenation Reactions Catalyzed by (*N*-Heterocyclic carbene)Pd(allyl)Cl Complexes. *J. Org. Chem.* **2004**, *69*, 3173−3180.
(74) Dehury, N.; Maity, N.; Tripathy, S. K.; Basset, J.-M.; Patra, S. Dinuclear Tetrapyrazolyl Palladium Complexes Exhibiting Facile Tandem Transfer Hydrogenation/Suzuki Coupling Reaction of Fluoroarylketone. *ACS Catal.* **2016**, *6*, 5535−5540.
(75) Viciu, M. S.; Grasa, G. A.; Nolan, S. P. Catalytic Dehalogenation of Aryl Halides Mediated by a Palladium/Imidazolium Salt System. *Organometallics* **2001**, *20*, 3607−3612.
(76) Guiral, V.; Delbecq, F.; Sautet, P. Hydride Transfer Reduction of Carbonyls by a Rhodium(I) Complex: A Theoretical Study. 1. The Two-Step Mechanism. *Organometallics* **2000**, *19*, 1589−1598.
(77) Hughes, R. P.; Kovacik, I.; Lindner, D. C.; Smith, J. M.; Willemsen, S.; Zhang, D.; Guzei, I. A.; Rheingold, A. L. Unusual Reactivity of "Proton Sponge" as a Hydride Donor to Transition Metals: Synthesis and Structural Characterization of Fluoroalkyl-(hydrido) Complexes of Iridium(III) and Rhodium(III). *Organometallics* **2001**, *20*, 3190−3197.
(78) Crabtree, R. H. The Organometallic Chemistry of the Transition Metals. In *The Organometallic Chemistry of the Transition Metals*, 6th ed.; Wiley: 2014.
(79) Liu, T.; Chai, H.; Wang, L.; Yu, Z. Exceptionally Active Assembled Dinuclear Ruthenium (II)-NNN Complex Catalysts for Transfer Hydrogenation of Ketones. *Organometallics* **2017**, *36*, 2914−2921.
(80) Suresh Kumar, B.; Puthiaraj, P.; Amali, A. J.; Pitchumani, K. Ultrafine bimetallic PdCo alloy nanoparticles on hollow carbon capsules: an efficient heterogeneous catalyst for transfer hydrogenation of carbonyl compounds. *ACS Sustainable Chem. Eng.* **2018**, *6*, 491−500.
(81) Miura, K.; Tomita, M.; Yamada, Y.; Hosomi, A. Indium-catalyzed radical reductions of organic halides with hydrosilanes. *J. Org. Chem.* **2007**, *72*, 787−792.
(82) Dehury, N.; Tripathy, S. K.; Sahoo, A.; Maity, N.; Patra, S. Facile tandem Suzuki coupling/transfer hydrogenation reaction with a bis-heteroscorpionate Pd−Ru complex. *Dalton Trans.* **2014**, *43*, 16597−16600.
(83) Prades, A.; Corberan, R.; Poyatos, M.; Peris, E. [$IrCl_2Cp^*$-(NHC)] Complexes as Highly Versatile Efficient Catalysts for the Cross-Coupling of Alcohols and Amines. *Chem. - Eur. J.* **2008**, *14*, 11474−11479.

https://dx.doi.org/10.1021/acs.organomet.0c00594
Organometallics XXXX, XXX, XXX−XXX